Available online at www.sciencedirect.com

SCIENCE DIRECT®

Diamond & Related Materials 14 (2005) 739–743

DIAMOND AND RELATED MATERIALS

www.elsevier.com/locate/diamond

Density-controlled carbon nanotubes

Cheng Hang Hsu*, Chia-Fu Chen, Chien-Chung Chen, Shih-Yu Chan

Department of Materials Science and Engineering, National Chiao Tung University, 1001 Ta Hsueh Road, Hsinchu 30050, Taiwan

Available online 29 January 2005

Abstract

We demonstrate that the field emission efficiency was greatly improved by reducing the density of carbon nanotubes (CNTs). In this study, catalyst composed of gold and nickel was deposited by e-gun evaporation before pre-treatment of furnace annealing. Carbon nanotubes were then grown on silicon substrate using bias-assisted microwave plasma chemical vapor deposition. Vertical aligned carbon nanotubes were grown with gas mixture of methane and hydrogen under external DC bias. The surface morphology and the tubular structure of carbon nanotubes were confirmed by electron microscopy and the density of carbon nanotubes could be controlled by the composition of the catalyst. The field emission properties were investigated through *I–V* measurement and the effects are discussed.

Keywords: Carbon nanotubes; Field emission; Microwave plasma chemical vapor deposition; Screening effect

1. Introduction

Carbon nanotubes have drawn a lot of attentions in decade due to their amazing physical and chemical properties as mechanical strength [1], heat conductance [2,3], aspect ratio, surface area and chemical stability. These superior abilities make CNT a good candidate for applications, for example, field effect transistors [4], Bio-Nanotube Membranes [5], fuel cells [6], and field emission devices [7]. Particularly, due to the advantages of high aspect ratio and electrical conductivity, relative low turn-on field, stable emission and life time can therefore be obtained for optimizing the performance of the field emission devices. Carbon nanotubes uses as field emitters have extensively been studied for years and probably to be the first commercial products [8] ever since their discovery.

It has been reported that the maximum current density of 10^9 A/cm^2 [9] can be transmitted by a CNT with contact electrodes and field emission from a single multi-walled CNTs reaches about 0.2 mA [10] which correspond to a current density of about 10^5 A/cm^2. These current densities were far beyond the requirement for practical field emission applications [11] and were hard to accomplish. Efforts have been made to improve the filed emission efficiency of CNTs, which includes purification [12] or doping [13], but the most effective ways are decreasing the density of the CNTs [14–16]. Methods like screen printing, anodic aluminium oxide (AAO) [17] and plasma etching [18,19] were used to adjust the field emission behaviour while complicated procedures generates more problems. It has been reported that the density of CNTs plays a significant role in the field emission behaviours, and theoretical value of the optimal CNTs' density was calculated as 2.5×10^7 emitters/cm^2 [15]. The screening effect varies with the CNTs' density drastically and the field enhancement is changed. In this study, CNTs' density can be tuned by varying the catalyst's composition or size and the density effect is confirmed experimentally. By directly changing the catalyst composition, it is possible to simplify the field emission devices processes.

2. Experimental details

Mirror-polished n-type, (100) oriented Si wafers with resistivity of 4.5–5.5 Ω/cm were cleaned by standard cleaning process to remove contaminations. Wet oxidation

* Corresponding author. Tel.: +886 3 5712121 ext. 55346; fax: +886 35724727.

E-mail address: jhh.mse92g@nctu.edu.tw (C.H. Hsu).

0925-9635/$ - see front matter © 2005 Elsevier B.V. All rights reserved.
doi:10.1016/j.diamond.2004.12.006

was then carried out using a high-temperature furnace system (model ASM LB-45) to form a layer of SiO_2 with thickness of 300 Å in order to prevent silicide formation between silicon and nickel. After that, nickel and gold film with total thickness of 200 Å was deposited sequentially on SiO_2 using an E-Gun Evaporator (model ULVAC EBX-10C, Japan). The specimen was then introduced into a programmable furnace and anneals at a temperature of 900 °C and kept for 2 h under argon atmosphere and then cooled to room temperature.

The pre-treated substrates underwent bias-assisted microwave plasma chemical vapor deposition to grow the CNTs. The microwave power was maintained at 400 W with an external negative DC voltage supplied to the substrate. The total pressure in the chamber was kept at 2000 Pa with reactive gas of a mixture with H_2/CH_4=40:10 introduced into the quartz chamber. The synthesis temperature was about 700 °C, as measured with an IR thermometer (Minolta TR-630).

After deposition, the CNTs were characterized by scanning electron microscope (SEM; JEOL JSM-6500F) with an acceleration voltage of 15 kV to observe the surface morphology. High resolution transmission electron microscopy (HR-TEM; Philips Tecnai 20) operating at 200 kV and Energy-Dispersive Spectrometry (EDS) was used to observe the nanostructure and the composition of the CNTs. The *I–V* measurement was taken at a pressure of 10^{-4} Pa with an indium–tin–oxide (ITO) glass as anode.

3. Results and discussion

It was shown in Fig. 1 that the surface roughness increased and the catalyst film tends to form spherical particles as the composition of gold increases due to relief of surface energy after furnace annealing. The catalyst particles gradually increased their size from flat surface to hundreds of nanometers in diameter. The increasing gold content leads to the decreasing nickel–gold alloy melting point and thus the particle sizes were increased. It can be seen from the Ni–Au phase diagram that nickel and gold tend to dissolve to each other easily, which means that the catalyst particle contains both nickel and gold. Although nickel and gold completely dissolve to each other at 900 °C and spinodal decomposition area exists, insufficient cooling rate contributing to nickel-rich and gold-rich domains exists which is the main idea of

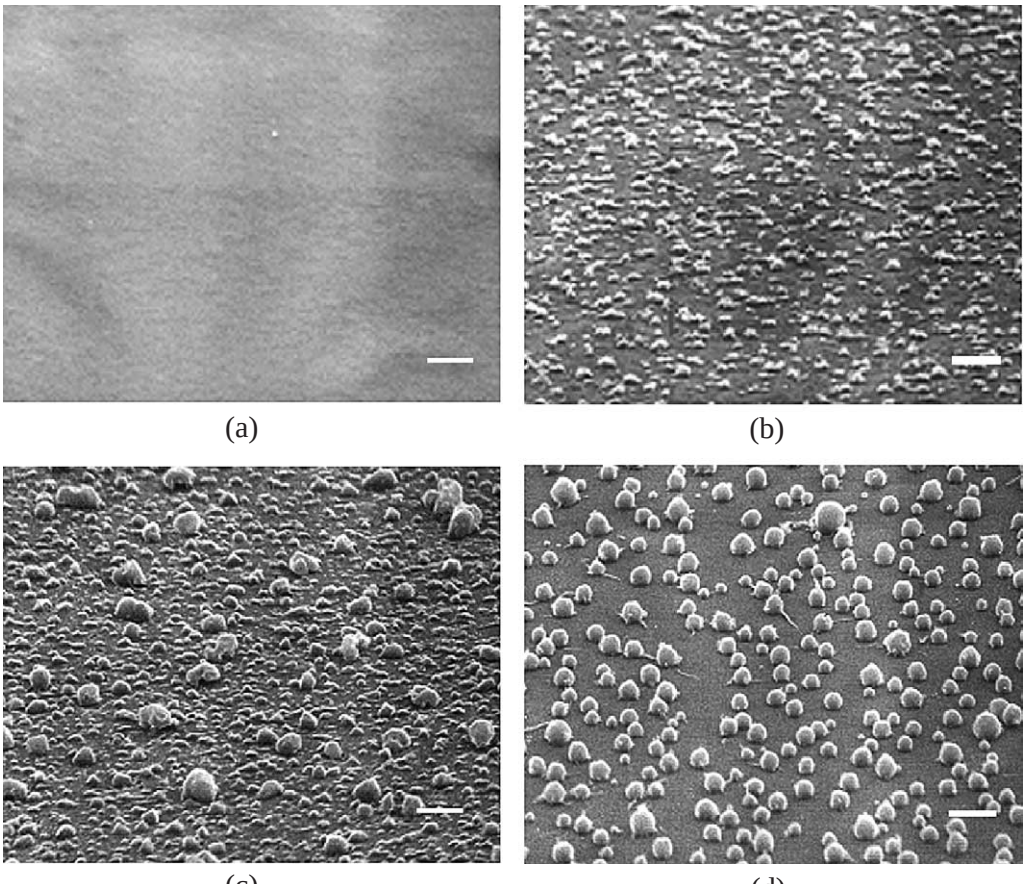

Fig. 1. Surface morphologies with different film composition of (a) Ni 170 Å, Au 30 Å (b) Ni 150 Å, Au 50 Å (c) Ni 130 Å, Au 70 Å (d) Ni 100 Å, Au 100 Å, which show different surface roughness. The scale bar in the image is 1 μm.

growing CNTs (the nickel-rich domain) or not (gold-rich domain).

The heat treated surface provided a template for further synthesis of different densities of CNTs. Fig. 2 shows the surface morphology of different CNTs densities with different heat treatment conditions. The CNTs grew to about 60 nm in diameter and several micrometers in length. Under the same conditions for CNTs' growth, it was found that the CNTs preferred to grew around the catalyst particles as shown in Fig. 1. It was reported [20] that the island model formatted by pre-treatment of the catalyst was favourable for continuous CNTs' film growth. The difference is that in this study, the gold or the Ni–Au solutions act as a CNTs growth inhibitor, which means the poor solvability of carbon in gold leads to a minor extrusion of carbon from the catalyst. The density therefore was reduced by the gold content which was unfavourable for CNTs growth and the increasing particle size which leads to fewer growth sites. Also, the bias in the microwave plasma chemical vapour deposition system provided a strong etching environment on the catalyst surface [21] which resisted the CNTs nucleation. However, it was found that the catalyst provided a shield of ion bombardment to the bottom of the particles near silicon surface and nickel-rich domains hence initiate the vapour–liquid–solid [22] growth of the CNTs. More precise analyses still need to be done in this complex system containing elements of silicon, oxygen, nickel and gold. The calculated CNTs densities of figure (a), (b), (c) and (d) are 2.2×10^{8} cm^{-2}, 6.1×10^{7} cm^{-2}, 4.7×10^{7} cm^{-2} and 3.3×10^{7} cm^{-2}, respectively.

Fig. 3(a and b) shows the TEM images of the CNTs obtained in Fig. 2(a and c), respectively. The tubular structure with the encapsulated catalyst could be verified. Fig. 3(a) shows the curved CNT where some curved CNTs on top of the vertical aligned CNTs could be found in Fig. 2(a). For the help of the EDS analysis in the TEM system, we found that the catalyst part of the CNTs contained detectable gold composition relative to the nickel. This phenomenon suggested that the gold content of the catalyst resulted in the formation of pentagon and heptagon carbon rings, which due to different carbon solvability and lead to the winding CNTs to compensate the strain [23]. However, the EDS analysis obtained from Fig. 3(a) shows no detectable gold content and was found in the catalyst and straight CNTs were formed by the applied negative bias voltages [24].

In order to examine the effects of CNTs' density on field emission properties, *I–V* measurement was utilized. Fig. 4 shows the *I–V* curves measured with different

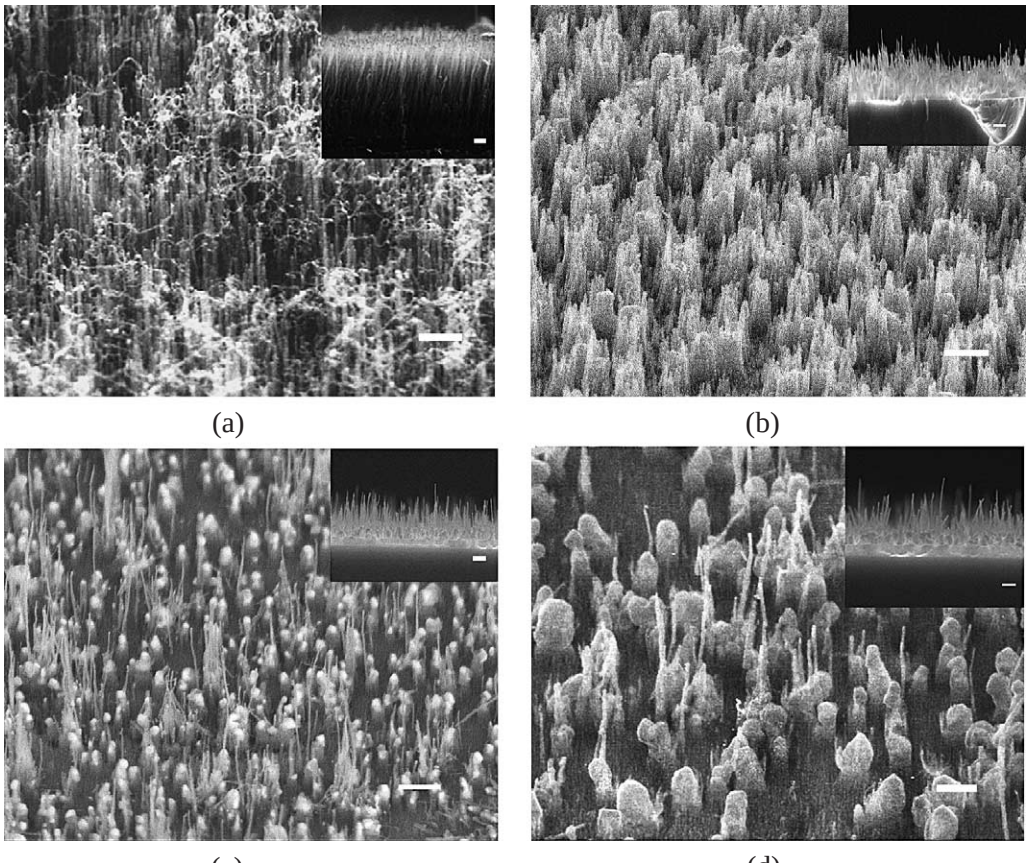

Fig. 2. SEM images of different density of CNTs (a) 2.2×10^{8} cm^{-2}, (b) 6.1×10^{7} cm^{-2}, (c) 4.7×10^{7} cm^{-2}, (d) 3.3×10^{7} cm^{-2} and the insets show the corresponding cross-section images. The scale bar in the image is 1 μm.

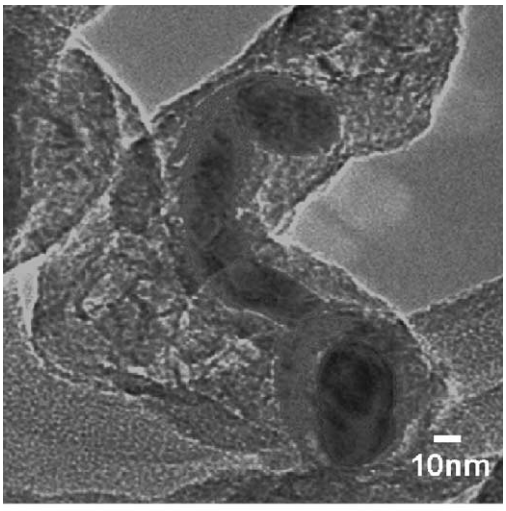

(a)

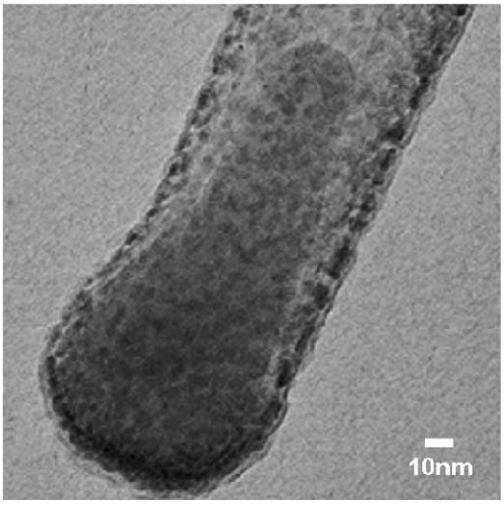

(b)

Fig. 3. TEM images of the CNTs showing (a) the curved CNT consisting of nickel and gold, (b) straight CNT consisting of nickel.

CNTs density. Apparently, field emission efficiency was enormously improved relatively to the sample whose continuous CNTs film was present. By decreasing the amount of CNTs, there was improvement in the emission current. The field emission efficiency should relate to two terms, in which dense CNTs will reduce the enhancement factor while, too low, the density will cause poor emission sites. The best density of CNTs was unable to be acquired from the plot yet in which the suggested value of 2.5×10^{7} cm^{-2} [15] is not attainable in this experiment.

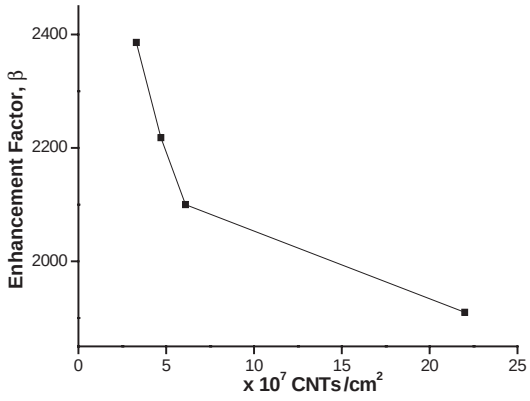

Fig. 5. Plot of field enhancement factor versus density of CNTs.

Fowler–Nordheim [25] equations have always been used to describe the relationship between the performance, geometrical parameters and material properties for field emission cases. Under the situation of the same material used, which means the work function is assumed to be identical, field enhancement factor or the geometrical term, β, is commonly introduced to characterize whether the performance is good or not. The larger the β is, the better the field emission properties will be. Fig. 5 shows the β value versus the CNTs' density. The enhancement factor increased exponentially from 1900 to 2400 with decreasing CNTs densities from 2.2×10^{8} cm^{-2} to 3.3×10^{7} cm^{-2}. It was found that the slope of the curve was nearly vertical when density of CNTs approached the calculated value of 2.5×10^{7} cm^{-2} from the simulation [15], and suggested a maximum enhancement factor can be obtained with the density.

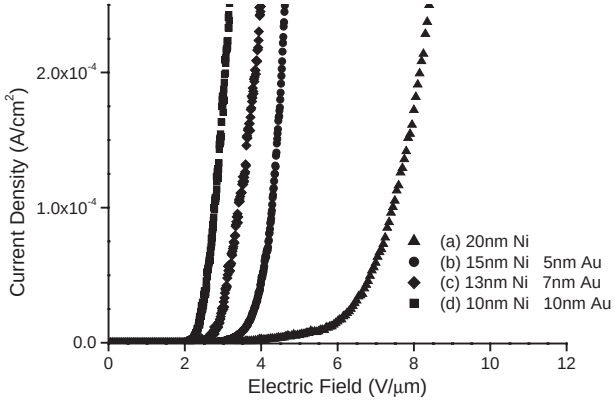

Fig. 4. Field emission from different densities of CNTs as shown in Fig. 2.

4. Conclusions

In this study, binary catalyst system with gold and nickel successfully inhibits the continuous film of CNTs formation using bias-assisted microwave plasma chemical vapor deposition. The vertical aligned CNTs can be grown under negative bias voltages and the gold composition contributed to the growth of the curved CNTs. The density of CNTs can be reduced to the value of 3.3×10^7 cm^{-2} by changing the composition and the heat treatment of the catalyst film. Field emission measurements demonstrate that the experimental value is very close to the reported one of 2.5×10^7 cm^{-2} and is possible for optimizing field emission efficiency for practical applications.

Acknowledgments

The authors would like to thank the National Science Council of the Republic of China under contract number NSC92-2216-E-009-007 for the financial help and the Wafer Works Corporation, Taiwan for the provision of silicon wafers.

References

[1] M.F. Yu, O. Lourie, M.J. Dyer, K. Moloni, T.F. Kelly, R.S. Ruoff, Science 287 (2000) 637.
[2] M.A. Osman, D. Srivastava, Nanotechnology 12 (2001) 21.
[3] J. Hone, M. Whitney, C. Piskoti, A. Zettl, Phys. Rev., B 59 (1999) R2514.
[4] W. Henk, Ch. Postma, Tijs Teepen, Zhen Yao, Milena Grifoni, Cees Dekker, Science 293 (2001) 76.
[5] Sang Bok Lee, David T. Mitchell, Lacramioara Trofin, Tarja K. Nevanen, Hans Söderlund, Charles R. Martin, Science 21 (2002) 2198.
[6] G. Che, B.B. Lakshmi, E.R. Fisher, C.R. Martin, Nature 393 (1998) 346.
[7] Shoushan Fan, Michael G. Chapline, Nathan R. Franklin, Thomas W. Tombler, Alan M. Cassell, Hongjie Dai, Science 22 (1999) 512.
[8] Q.H. Wang, A.A. Setlur, J.M. Lauerhaas, J.Y. Dai, E.W. Seelig, R.P.H. Chang, Appl. Phys. Lett. 72 (1998) 2912.
[9] Philip G. Collins, Michael S. Arnold, Phaedon Avouris, Science 292 (2002) 706.
[10] J.-M. Bonard, J.-P. Salvetat, T. Stöckli, L. Forr'o, A. Châtelain, Appl. Phys., A 69 (1999) 245.
[11] M. Kasu, N. Kobayashi, Appl. Phys. Lett. 76 (2000) 2910.
[12] C.M. Chen, M. Chen, F.C. Leu, S.Y. Hsu, S.C. Wang, S.C. Shi, C.F. Chen, Diamond Relat. Mater. 13 (2004) 1182.
[13] C.F. Chen, C.L. Tsai, C.L. Lin, Diamond Relat. Mater. 12 (2003) 1500.
[14] K.B.K. Teo, M. Chhowalla, G.A.J. Amaratunga, W.I. Milne, G. Pirio, P. Legagneux, F. Wyczisk, D. Pribat, D.G. Hasko, Appl. Phys. Lett. 80 (2002) 2011.
[15] L. Nilsson, O. Groening, C. Emmenegger, O. Kuettel, E. Schaller, L. Schlapbach, H. Kind, J.M. Bonard, K. Kern, Appl. Phys. Lett. 76 (2000) 2071.
[16] Y. Tu, Z.P. Huang, D.Z. Wang, J.G. Wen, Z.F. Ren, Appl. Phys. Lett. 80 (2002) 4018.
[17] J.S. Suh, K.S. Jeong, J.S. Lee, Appl. Phys. Lett. 80 (2002) 2392.
[18] C.Y. Zhi, X.D. Bai, E.G. Wang, Appl. Phys. Lett. 81 (2002) 1690.
[19] J.H. Choi, S.H. Choi, J.H. Han, J.B. Yoo, C.Y. Park, T. Jung, S. Yu, I.T. Han, J.N. Kim, Appl. Phys. Lett. 94 (2003) 487.
[20] Y.B. Zhu, W.L. Wang*, K.J. Liao, Y. Ma, Diamond Relat. Mater. 12 (2003) 1862.
[21] C.H. Hsu, S.C. Shi, C.F. Chen, Thin Solid Films (in press).
[22] Y. Saito, et al., Chem. Phys. Lett. 204 (1993) 277.
[23] Ph. Lambin, J.P. Vigneron, A. Fonseca, J.B. Nagy, A.A. Lucas, Synth. Met. 77 (1996) 249.
[24] C.L. Tsai, C.F. Chen, Diamond Relat. Mater. 12 (2003) 1615.
[25] R.H. Fowler, D.L. Nordheim, Roy. Soc. Proc., A 173 (1928).